0026-895X/88/020229-09$02.00/0
Copyright © by The American Society for Pharmacology and Experimental Therapeutics
All rights of reproduction in any form reserved.
MOLECULAR PHARMACOLOGY, 34:229–237

MOL PHARM

Kinetic and Equilibrium Studies of *Ah* Receptor-Ligand Binding: Use of [^{125}I]2-Iodo-7,8-dibromodibenzo-*p*-dioxin

CHRISTOPHER A. BRADFIELD, ANDREW S. KENDE, and ALAN POLAND

McArdle Laboratory for Cancer Research, University of Wisconsin, Madison, Wisconsin 53706 (C.A.B., A.P.) and Department of Chemistry, University of Rochester, Rochester New York 14627 (A.S.K.)

Received December 14, 1987; Accepted April 12, 1988

SUMMARY

In this report, we have used the radioligand [^{125}I]2-iodo-7,8-dibromo-dibenzo-*p*-dioxin to describe the kinetics of ligand binding to the *Ah* receptor prepared from C57BL/6J mouse liver. The higher specific activity of this radioligand (2176 Ci/mmol), compared with the usual tritiated ligand [1,6-^{3}H]2,3,7,8-tetrachlorodibenzo-*p*-dioxin (58 Ci/mmol) permitted the study of ligand-receptor interactions at much lower component concentrations. For this radioiodinated ligand, Scatchard analysis of saturation binding curves, determined at six different protein concentrations, indicated that the apparent equilibrium dissociation constant, K_D, was directly related to the dilution of the receptor preparation; for example, at 1160 μg of protein/ml, $K_D = 1.6 \times 10^{-10}$ M; at 36 μg of protein/ml, $K_D = 1.2 \times 10^{-11}$ M. Extrapolation of this function to infinite receptor dilution yielded $K_D = 6 \times 10^{-12}$ M. The addition of 70 μg/ml of bovine serum albumin to a receptor preparation of 30 μg of protein/ml produced a 10-fold decrease in the slope of the Scatchard plot (i.e., 10-fold increase in the apparent K_D). Conversely, enrichment of the receptor by high performance liquid chromatography led to an increased slope and thus decreased estimate of K_D. The association rate constant (k_1), calculated from the integrated second-order rate equation, was 2.8×10^{10} M^{-1} hr^{-1} and, from the initial velocity equation, had a value of 5.25×10^{10} M^{-1} hr^{-1}. The dissociation rate constant was biphasic, consisting of a predominant fast component with a rate constant of 0.36 hr^{-1} (k_{-1}) and a slower component with a rate constant of 4.2–9.4 $\times 10^{-3}$ hr^{-1} (k_{-2}). Higher protein concentrations produced a decrease in estimates of k_1 but not k_{-1} or k_{-2}. The K_D determined from the ratio of the kinetic rate constant, $k_{-1}/k_1 = 6.9 \times 10^{-12}$ M, is in excellent agreement with that derived from the results of equilibrium binding experiments extrapolated to infinite dilution, $K_D = 6 \times 10^{-12}$ M. The decrease in K_D, observed in equilibrium binding studies upon dilution of the receptor preparation, is best explained by a more accurate classification of "free" radioligand at lower protein concentrations. Finally, ligand binding to the *Ah* receptor is best described by a two-step process, the formation of an initial complex, characterized by rapid ligand dissociation, which undergoes transformation to a second distinct complex displaying a much slower ligand dissociation rate.

Planar halogenated aromatic hydrocarbons elicit a variety of biological effects, including induction of cytochrome P-450 isozymes, epidermal hyperplasia and metaplasia, thymic involution, teratogenesis, tumor promotion, and lethality (1). These diverse biological responses are believed to arise from the altered gene expression that is consequent to the high affinity, stereospecific binding of planar halogenated aromatic hydrocarbons to a soluble protein known as the *Ah* receptor (1, 2).

Like the steroid hormone receptors, the *Ah* receptor is routinely found in the high speed supernatant fraction ("cytosol") of tissue homogenates. After ligand binding and a poorly defined "transformation"[1] step, the ligand-receptor complex displays an increased affinity for polyanions, such as DNA (3–6), and functions as a transcriptional activator (7, 8). The *Ah* receptor also bears many physicochemical similarities to steroid hormone receptors, including a high molecular weight "aggregate" form in low salt buffers (M_r 2.5–2.8 $\times 10^5$) that dissociates to a low molecular weight "monomeric subunit" form in high salt buffers (M_r approximately 1×10^5) (9). For the *Ah* receptor present in the hepatic cytosol of the C57BL/6 mouse and the Sprague-Dawley rat estimates of sedimentation coefficients,

This paper is dedicated to Dr. Elizabeth Miller.

This work was supported in part by the National Institute of Environmental Health Science Grant ES-01884, National Cancer Institute Core Grant-07175, and National Cancer Institute Postdoctoral Training Grant T32-CA09020.

[1] Receptor transformation is defined in this report as an alteration in the physiochemical nature of the ligand-receptor complex, which results in an increased affinity for DNA or other polyanionic matrices.

ABBREVIATIONS: TCDD, 2,3,7,8-tetrachlorodibenzo-*p*-dioxin; MOPS, 3-(*N*-morpholino)propanesulfonic acid; K_D, equilibrium dissociation constant; [*L*], concentration of unbound ligand; [*R*], concentration of unliganded receptor; [*LR*], concentration of receptor-ligand complex; $[LR]_e$, receptor-ligand complex at equilibrium; [*LR'*], concentration of activated RL complex; $[L]_T$, total radioligand concentration; $[R]_T$, total receptor concentration; B_{max}, receptor concentration per ml; k_1, second-order rate constant of association; k_{-1}, fast component dissociation rate constant; k_{-2}, slow component dissociation rate constant; HPLC, high performance liquid chromatography; TEA, triethylamine; $t_{1/2}$, half-life of dissociation; ASPPT, 40–55% ammonium sulfate precipitate; BCA, bicinchoninic acid; BSA, bovine serum albumin; DMSO, dimethyl sulfoxide.

MOLECULAR PHARMACOLOGY
aspet
Downloaded from molpharm.aspetjournals.org at Universidade do Estado do Rio de Janeiro on December 4, 2012

MOL PHARM

MOLECULAR PHARMACOLOGY

Stokes radii, molecular weights, and frictional and axial ratios (9) are all within the ranges described for steroid hormone receptors (e.g., for the low salt aggregate form of steroid hormone receptors the ranges reported are: sedimentation coefficient, 8–10 S; Stokes radius, 7–10 nm; molecular weight, 2–3.5 × 10^5; frictional ratio, 1.45–2; and axial ratio 8–20; for a complete listing see Ref. 10).

We recently reported the synthesis and use of an ^{125}I-labeled azidodibenzo-*p*-dioxin as a photoaffinity ligand for the *Ah* receptor (11). The use of ^{125}I-labeled dioxin congeners is appealing because of their higher specific activity and counting efficiency compared with tritiated ligands. We now report the synthesis of a reversible radioligand, [^{125}I]2-iodo-7,8-dibromodibenzo-*p*-dioxin, and its use to characterize the ligand binding kinetics of the murine hepatic *Ah* receptor.

Materials and Methods

Reagents

TCDD was a gift of Dow Chemical Co. (Midland, MI); 2,3,7,8-tetrachlorodibenzofuran was a gift from Dr. David Firestone (Food and Drug Administration, Washington, D.C.). Activated charcoal, grade PX-21, was a gift from Amoco Research Corp. (Chicago, IL). Bacto-Gelatin was from Difco Laboratories (Detroit, MI). Magnesium sulfate was from Fisher Scientific Co. (Fair Lawn, NJ). Ammonium sulfate (ultra-pure) was from Schwarz/Mann (Cambridge, MA). Methanol (HPLC grade) was from Burdick and Jackson Laboratories, Inc. (Muskegan, MI). Glycerol was from J. T. Baker (Phillipsburg, NJ). EDTA was from EM Scientific (Cherry Hill, NJ). Carrier-free Na^{125}I (NE2-033L) was from New England Nuclear (North Billerica, MA). BSA, dithiothreitol, β-mercaptoethanol, sodium azide, chloramine T, MOPS (free acid and sodium salt), TEA, and TEA hydrochloride were purchased from Sigma Chemical Co. (St. Louis, MO). Dichloromethane (reagent grade), tetrahydrofuran (anhydrous, 99.9% pure), *n*-butyl nitrite (97% pure), *p*-dioxane (anhydrous 99+% pure), and dimethyl sulfoxide (anhydrous, 99% pure, stored under N_2 gas) were purchased from Aldrich Chemical Co. (Milwaukee, WI). BCA Protein Assay Reagent was purchased from Pierce Chemical Co. (Rockford, IL).

Buffers

MN represents the stock buffer which contains 25 mM MOPS and 0.02% sodium azide, pH 7.5 (at 4°). MEN is the stock buffer plus 1 mM EDTA. MβENG and MDENG represent MEN with the addition of 10% (w/v) glycerol, plus the addition of either 10 mM β-mercaptoethanol or 1 mM dithiothreitol.

Radiosynthesis of [^{125}I]2-iodo-7,8-dibromodibenzo-*p*-dioxin

The synthesis was performed in a room dedicated to radiosynthesis, equipped with a high flow chemical hood, with the use of sealed vials and airtight syringes to minimize escape of radioiodine. The entire procedure was monitored with a γ-radiation detector.

Synthesis of [^{125}I]2-amino-3-iodo-7,8-dibromodibenzo-*p*-dioxin (Fig. 1). To 5 mCi of carrier-free Na^{125}I (≥350 mCi/ml in 6 mM NaOH, ≤15 μl of water) in a septum-sealed conical vial was added 2.5 nmol of 2-amino-7,8-dibromodibenzo-*p*-dioxin (11) in 25 μl of methanol, 1.13 μmol of sulfuric acid in 10 μl of methanol/water (9:1), and 25 nmol of chloramine T in 5 μl of methanol (12). The iodination reaction was complete in 30 min and terminated by the addition of 500 μg of sodium metabisulfite and 5 μmol of sodium hydroxide in 35 μl of water. The reaction product, [^{125}I]2-amino-3-iodo-7,8-dibromodibenzo-*p*-dioxin, was extracted with 250 μl of dichloromethane with the use of a vortex mixer (30 sec). The organic phase was aspirated into a syringe (gas syringe, pressure-locked plunger tip, P010032; Pierce Chemical Co., Rockford, IL) transferred to a 1-ml sealed conical vial (Reacti-vial 13221, Pierce Chemical Co.) containing 10 mg of magnesium sulfate, 75 μl of dichloromethane, and a microstirring bar, and the mixture was stirred for 45 min to dry the organic phase.

[^{125}I]2-iodo-7,8-dibromodibenzo-*p*-dioxin was formed from [^{125}I]2-amino-3-iodo-7,8,dibromodibenzo-*p*-dioxin by generation of the aryldiazonium salt, which produces the aryl radical with subsequent abstraction of hydrogen from tetrahydrofuran to form the deaminated product (13). This was accomplished as follows. The dried dichloromethane solution was aspirated and transferred to a 1-ml conical vial containing 250 μl of anhydrous tetrahydrofuran and 67 μmol of *n*-butyl nitrite. The reaction mix was then heated at 55° with stirring. After 15 min, the vial was opened and the solvent evaporated, with heating, under a stream of nitrogen gas, venting the vial into a funnel (2 cm diameter) attached to two serially connected charcoal filters in line with negative airflow. This system trapped most of the volatile radioiodine in the first charcoal filter and minimized release into the laboratory hood ventilation system. The reaction mix solute was dissolved in 50 μl of methanol/water (92:8) and the ^{125}I-labeled product purified by HPLC as detailed below.

Analysis and Purification of the Radioligand

Unlabeled 2-iodo-7,8-dibromodibenzo-*p*-dioxin, synthesized as above on a milligram scale, was used as an analytical standard. The unlabeled compound was characterized by 1) low resolution mass spectrometry: *m/e* (more than 40% of the base peak) 467.9 (100% M^+), 469.9 (46%), 466 (50%), 71 (55%), and 43.1 (60%); and 2) reverse phase HPLC; using a C-18 column, 4.6 × 250 mm, 5 μm particle (Altex Scientific Inc., Berkeley, CA), and an isocratic solvent system (methanol/water, 92:8) with a flow rate at 1 ml/min. The compound was detected by its UV absorbance at 254 nm and eluted with a retention time of 24 min.

The radiolabeled reaction mix was subjected to HPLC separation as above. Approximately 60% of the radioactivity injected eluted with a UV absorption peak that had a retention time identical to that of the unlabeled compound (i.e., 24 min). In this methanol/water HPLC system, the potentially significant reaction product contaminants, 2-amino-7,8-dibromodibenzo-*p*-dioxin, 2-iodo-3-amino-7,8-dibromodibenzo-*p*-dioxin, and 2,3-dibromodibenzo-*p*-dioxin, elute with retention times of 6.8, 11.6, and 13.0 min, respectively. Reinjection of the 24-min eluate (from above) also cochromatographs with authentic 2-iodo-7,8-dibromodibenzo-*p*-dioxin using an 9:1 acetonitrile/water isocratic solvent system (retention time, 22 min; 98% radiochemical purity). The overall yield of radioligand, judged by incorporation of ^{125}I into the purified product, ranges from 40 to 50%. The specific activity was assumed to be equivalent to that of carrier-free Na^{125}I, (2176 Ci/mmol, 4,831 dpm/fmol). The radioligand was stored at 6 × 10^8 dpm/ml in *p*-dioxane in a capped test tube protected from light. For use in binding experiments, an aliquot of the stock solution was dried under a stream of nitrogen gas and redissolved in DMSO at the appropriate concentration.

Receptor Preparation

Cytosol. C57BL/6J mice were purchased from The Jackson Laboratory (Bar Harbor, ME) and bred in our laboratory. Adult male and female mice were killed by cervical dislocation and their livers were removed, rinsed with ice-cold KCl (150 mM), homogenized in 9 volumes of MβENG buffer, and centrifuged at 10,000 × *g* for 20 min at 4°. The postmitochondrial supernatant was carefully removed to avoid contamination by the surface lipid layer and subjected to centrifugation at 105,000 × *g*. The supernatant (approximately 10 mg of protein/ml) was

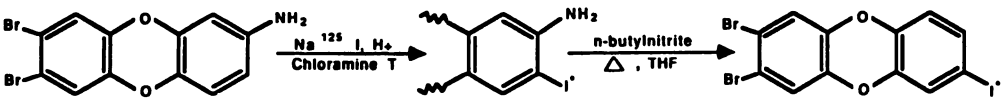

Fig. 1. Radiosynthesis of [^{125}I]2-iodo-7,8-dibromodibenzo-*p*-dioxin. *THF*, tetrahydrofuran.

Downloaded from molpharm.aspetjournals.org at Universidade do Estado do Rio de Janeiro on December 4, 2012

separated from surface lipids and the microsomal pellet and stored at −80° for use in binding experiments or until processed further.

ASPPT. The frozen cytosolic fraction was thawed and placed in an ice bath with slow stirring. A saturated solution of ammonium sulfate in MEN buffer was added to the cytosolic preparation, to a final concentration of 40%, over a period of 30 min and stirred for an additional 30 min. The solution was centrifuged at 10,000 × *g* for 20 min, and the supernatant fraction was removed, slowly brought to an ammonium sulfate concentration of 55%, stirred for an additional 30 min, and centrifuged at 10,000 × *g*, and the supernatant was discarded. The ASPPT was resuspended in 55% ammonium sulfate in MβEN, and aliquots equivalent to 0.5 g wet weight of liver (15 mg of protein) were placed in 12 × 75 mm borosilicate tubes (VWR Scientific, San Francisco, CA) and spun at 5000 × *g*. The supernatant was removed by careful aspiration, and the pellets were stored in stoppered tubes at −80° until use.

HPLC-anion exchange-enriched receptor preparation. HPLC-anion exchange chromatography was performed on a Mono-Q HR 5/5 column (5 × 50 mm; Pharmacia, Uppsala, Sweden). All column parts, external tubing, injection loop, and buffers were placed on ice during the entire run. The HPLC instrumentation was identical to that outlined in the purification of the radioligand (above). The sample (ASPPT fraction, 200–900 μg of protein) was dissolved in 1–2 ml of 20 mM TEA buffer pH 7.5 (4°) and injected into a 2-ml sample loop. The elution buffers used were the following: buffer A, 20 mM TEA, pH 7.5; and buffer B, 20 mM TEA, pH 7.5, plus 500 mM NaCl. The linear gradient program ran from 100:0 (A:B) to 40:60 over 8 min, then to 10:90 over 10 min, followed by isocratic elution (10:90) for 5 min. The 16–18-min fractions were collected and pooled for use in binding studies. These fractions appear at the beginning of a large UV-absorbing peak and thus some variation in purification was observed between runs. Protein concentrations were determined by the method of Warburg and Christian (14) or by the use of BCA Protein Assay using BSA as standard.

Binding Experiments

Binding experiments were carried out at 4°. The frozen ASPPT pellets or cytosolic fractions were dissolved and diluted in ice-cold MDENG buffer to the appropriate protein concentration. The radioligand and the competing unlabeled ligand (2,3,7,8-tetrachlorodibenzofuran) were dissolved in DMSO and added to the buffer/receptor solution so that the final concentration of solvent was 6 μl of DMSO per ml of buffer. Binding reactions were performed in 1.0-ml volumes (12 × 75 mm borosilicate test tubes), or in 50-ml volumes (Ehrlenmeyer flasks), from which 1.0-ml samples were transferred to the smaller tubes. The binding reaction was terminated by the addition of a 0.5-ml volume of an ice-cold charcoal/gelatin suspension (3%/0.3% in MN buffer). The suspension was then stirred vigorously on a vortex mixer (2 sec), followed by incubation for 10 min at 4°. The charcoal/gelatin was then sedimented at 2000 × *g* for 10 min at 4°. A 1.0-ml aliquot of the supernatant fraction of each tube was transferred to 12 × 75 mm polypropylene tubes (for higher counting efficiency, 75%), and the bound radioligand was quantified in a MINAXI Series-5000 γ-counter (United Technologies/Packard Instrument Co., Downers Grove, IL). Sample counting times were adjusted to achieve a counting error of 3%.

Total radioligand, $[L]_T$, was defined as the concentration of radioligand in solution after the 16-hr incubation. Total radioligand bound was defined as the radioligand in solution after charcoal adsorption. Nonspecific binding was defined as the amount of radioligand bound in the presence of a 200-fold molar excess of 2,3,7,8-tetrachlorodibenzofuran. Specific binding was defined as the difference between total radioligand bound and radioligand nonspecifically bound. Unbound ("free") radioligand was defined as the difference between total radioligand and total bound radioligand.

Software

Weighted nonlinear curve-fitting estimates of binding parameters were determined as described (15, 16) using a commercially available software package for the IBM-PC (Kinetic, EBDA, Ligand, Lowry; Elsevier Biosoft, Cambridge, England).

Results

Equilibrium binding analysis. Equilibrium saturation binding of [^{125}]2-iodo-7,8-dibromodibenzo-*p*-dioxin to the hepatic *Ah* receptor of C57BL/6J mice, determined at three different protein concentrations, is shown in Fig. 2. Analysis of saturation binding curves by the method of Scatchard (17) is presented in Figure 3 and Table 1. With progressive 2-fold dilutions of the receptor preparation, the estimate of maximal binding sites per ml, B_{max} (x axis intercept), shows approximately 2-fold decreases, i.e., B_{max}/mg of protein remains constant (Table 1; Fig. 3). Unexpectedly, the slopes of the Scatchard plots ($-1/K_D$) increased from 2.6- to 1.2-fold with each 2-fold dilution (i.e., the estimate of K_D decreased from 1.6×10^{-10} to 1.2×10^{-11} M, as the protein concentration decreased from 1160 to 36 μg/ml).

Hill coefficients were 1.0 at all receptor dilutions, indicating that site-site cooperatively did not contribute to the increase in the slope of Scatchard plots observed with dilution (18). Scatchard and Hill analyses of saturation binding data were reproducible and of good linear fit, with coefficients of variation below 30% and with correlation coefficients of at least 0.96 (Table 1).

Regression analysis of the relationship between the protein concentration of the ASPPT and the estimate of K_D as determined by Scatchard analysis suggested a simple linear function (Fig. 4). Extrapolation of the least squares fit of the line to the y intercept (infinite dilution of protein) yielded an estimate of K_D of $6 \pm 3 \times 10^{-12}$ M.

Two experiments were conducted to describe more clearly the relationship between protein concentration and the increase in apparent binding affinity that was observed with dilution. First, when the *Ah* receptor concentration (B_{max} mg of protein) in the ASPPT fraction was enriched 5- to 9-fold by HPLC-anion exchange chromatography, the estimated K_D was approximately 4-fold lower than the K_D determined on the corresponding ASPPT fraction (Table 1; compare 20 mg/ml wet weight values). Second, saturation binding was described on an ASPPT preparation (30 μg/ml) in the absence or presence of 70 μg/ml of a highly purified protein, BSA (Fig. 5). Scatchard analysis of the binding data described a 10-fold increase in the apparent K_D when BSA was present. Despite the large effect of BSA on the apparent K_D, the estimate of B_{max} was only slightly increased in the presence of the additional protein, approximately 1.3-fold. It should be noted that this ASPPT preparation was from a different batch than that used to generate the data in Table 1 and Figs. 2, 3, and 4. This preparation yielded a slightly greater receptor concentration per milligram of protein.

Binding kinetics. For a simple bimolecular reaction governed by the law of mass action, the K_D of ligand binding is equal to the rate constant of ligand-receptor dissociation divided by the second-order rate constant of ligand-receptor association:

$$R + L \underset{k_{-1}}{\overset{k_1}{\leftrightarrows}} RL \qquad (1)$$

and

$$K_D = \frac{k_{-1}}{k_1} \qquad (2)$$

MOL PHARM
MOLECULAR PHARMACOLOGY
aspet
Downloaded from molpharm.aspetjournals.org at Universidade do Estado do Rio de Janeiro on December 4, 2012

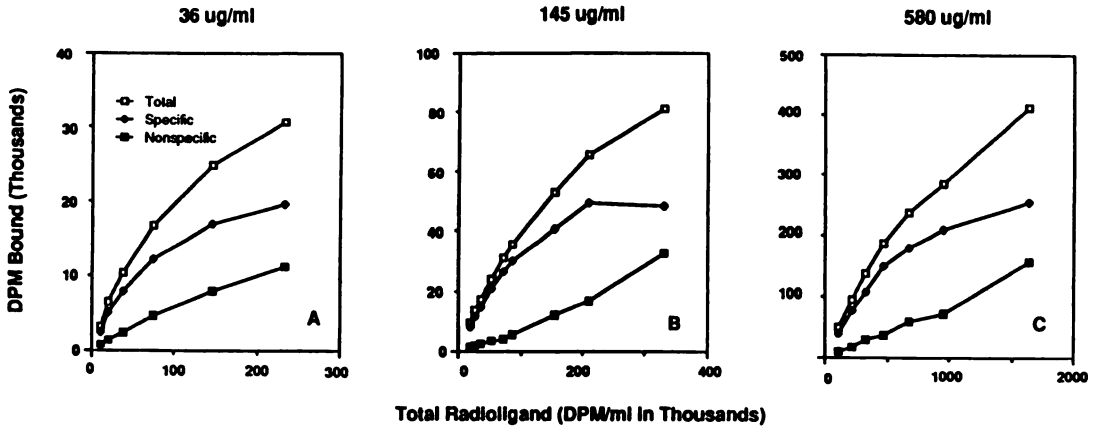

Fig. 2. Equilibrium binding of [^{125}I]2-iodo-7,8-dibromodibenzo-*p*-dioxin. The receptor preparation [ASPPT, 36 (A), 145 (B), or 580 (C) μg of protein/ml] was incubated at 4° for 16 hr, with concentrations of radioligand ranging from 2.5 to 250 fmol/ml. Total, specifically bound, and nonspecifically bound radioligand were determined as outlined in Materials and Methods. Each *point* represents the average of duplicate determinations.

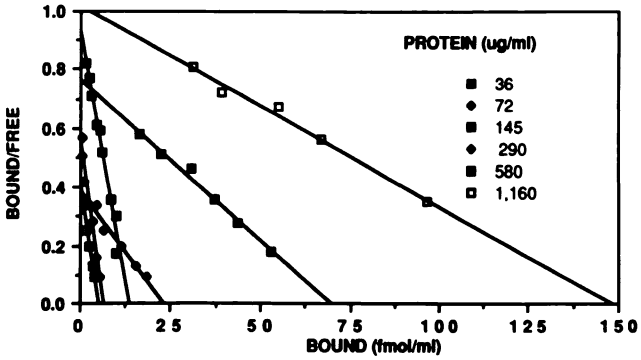

Fig. 3. Scatchard analysis of equilibrium binding data generated at various dilutions of receptor. Equilibrium saturation binding curves of [^{125}I]2-iodo-7,8-dibromodibenzo-*p*-dioxin were determined at various dilutions of the ASPPT fraction (as described in Fig. 2). The binding parameters K_D (−1/slope of the line) and B_{max} (receptor concentration/ml; the *x* intercept) were calculated from a weighted least squares fit of a plot of specifically bound radioligand/free radioligand versus specifically bound radioligand (16, 17). When more than two plots were generated at a given protein concentration, the plot that yielded the median K_D value was chosen for presentation.

Eq. 2 provides an estimate of the K_D, independent of that calculated from equilibrium binding studies.

Association rate constant. The rate constant of association was calculated from the time course of ligand-receptor binding, via the integrated second-order rate equation, as described by Weiland and Molinoff (19):

$$\ln\left[\frac{[\mathrm{LR}]_e\,[[\mathrm{L}]_T - [\mathrm{LR}]\,[\mathrm{LR}]_e/[\mathrm{R}]_T]}{[\mathrm{L}]_T[[\mathrm{LR}]_e - [\mathrm{LR}]]}\right] = k_1 t\left[\frac{[\mathrm{L}]_T[\mathrm{R}]_T}{[\mathrm{LR}]_e} - [\mathrm{LR}]_e\right] \quad (3)$$

Substitution of $\ln Y$ for the left side of the equation and rearrangement yields the equation of a straight line, with slope $\ln Y$/time. Thus, k_1 can be calculated from the relationship:

$$k_1 = \frac{\text{slope}}{\frac{[L]_T[R]_T}{[LR]_e} - [LR]_e} \quad (4)$$

This method allows determination of k_1 from estimates of the concentrations of total ligand, $[L]_T$, total receptor, $[R]_T$ (obtained from Scatchard analysis), ligand-receptor complex at equilibrium, $[LR]_e$, and ligand-receptor complex, $[LR]$, at various time intervals, t. The advantage of this method is that no constraints are placed upon the concentrations of ligand or receptor used in the binding studies. By this method, dilution of the protein concentration by 18-fold resulted in a 37-fold increase in the calculated rate constant of association (k_1 = 7.6 × 10^8 to 3.0 × 10^{10} M^{-1} hr^{-1}; Fig. 6, A and B, and Table 2). In contrast, at a fixed protein concentration a 13-fold change in total radioligand concentration did not alter the association rate constant (i.e., k_1 = 3.0 and 2.6 × 10^{10} M^{-1} hr^{-1}; Fig. 6, B and C, and Table 2).

The association rate constant was also estimated from the initial binding velocities (v_0) under conditions in which $[L]_T$ and $[R]_T \gg [LR]$, so the free radioligand and free receptor concentrations are approximated by $[L]_T$ and $[R]_T$, respectively.

TABLE 1

Summary of saturation binding experiments performed on the *Ah* receptor at various protein concentrations

The saturation binding isotherms for the radioligand and *Ah* receptor in hepatic cytosol, the ASPPT fraction of cytosol, and the HPLC-enriched preparation of the ASPPT fraction were determined over a range of protein concentrations. The binding parameters K_D, and B_{max} were calculated by Scatchard analysis of binding data as described in the legend to Fig. 2 or by Hill analysis of binding data as described (18). Values represent the mean ± the standard deviation, except in the case of a single data point or duplicate data points, for which only the mean is given. Correlation coefficients were at least 0.96 for both Scatchard and Hill plots. The standard deviation of the Hill coefficient did not exceed 0.02.

Equivalent wet weight	Protein	K_D	B_{max}	Hill coefficient	Number of experiments
mg/ml	*μg/ml*	*pM*	*fmol/mg of protein*		
ASPPT					
1.25	36	12	141	1.0	1
2.5	72	14 ± 4	114 ± 21	1.00	5
5	145	19 ± 3	110 ± 14	0.97	4
10	290	49 ± 9	121 ± 7	0.98	3
20	580	92	121	0.98	1
40	1160	160	131	0.98	2
HPLC-Enriched					
6.7	8	11	780	1.00	1
14	9	12	611	0.99	1
20	25	22	684	0.98	1
30	48	22	1100	0.98	1
Cytosol					
0.62	42	7	95	1.00	1
1.25	85	13	113	1.00	2
2.5	170	24	80	0.99	1

MOL PHARM
MOLECULAR PHARMACOLOGY
aspet
Downloaded from molpharm.aspetjournals.org at Universidade do Estado do Rio de Janeiro on December 4, 2012

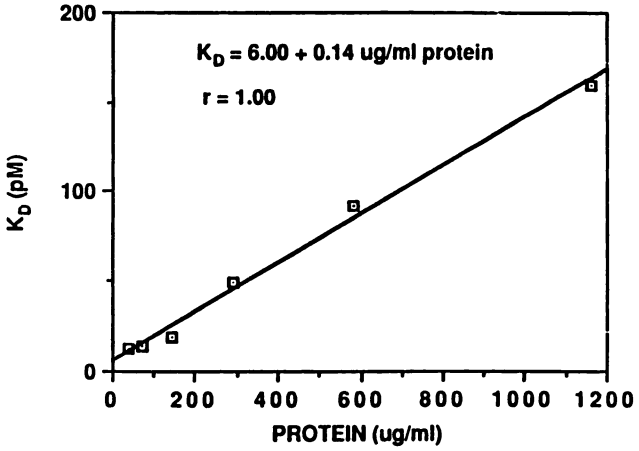

Fig. 4. The apparent K_D as a function of protein concentration. The apparent K_D, calculated from Scatchard analysis of radioligand binding to the ASPPT fraction, plotted as a function of the protein concentration (μg/ml). The data were fit to the equation of a straight line by the method of least squares. The equation of the line is inset. *r*, correlation coefficient.

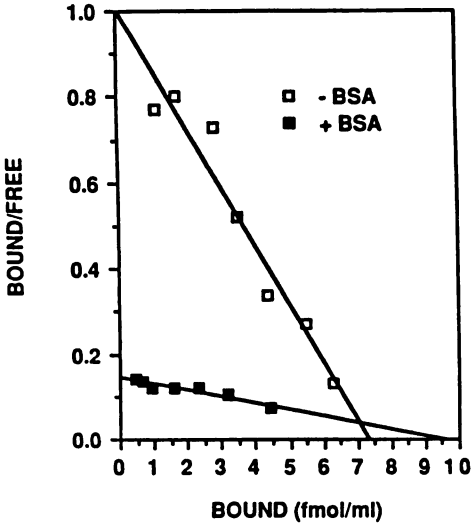

Fig. 5. The effect of BSA on the slope of the Scatchard plot. Equilibrium saturation binding curves were generated, as described in Fig. 3, for an ASPPT sample of 30 μg of protein/ml with and without the addition of 70 μg/ml BSA. Calculated binding parameters: plus BSA, $K_D = 6.3 \times 10^{-11}$ M, B_{max} = 9.2 fmol/ml; without BSA, $K_D = 7.3 \times 10^{-12}$ M, B_{max} = 7.4 fmol/ml.

where:

$$v_0 = k_1 [R]_T[L_T] \quad (5)$$

rearranging gives:

$$k_1 = v_0/[R]_T[L]_T \quad (6)$$

Plotting initial binding velocity as a function of receptor or radioligand concentration, with the other variable fixed, allows the determination of k_1.

A plot of initial binding velocity versus receptor concentration yielded a hyperbolic plot (Fig. 7A). The correlation coefficient of the plot (for a linear fit) using all data points presented is 0.94. By elimination of the values obtained above a receptor concentration of 1×10^{-11} M and inclusion of the theoretical *y* intercept of (0,0), a correlation coefficient of 0.99 is obtained and an association rate constant of 5.5×10^{10} M^{-1} hr^{-1} is calculated (i.e., calculation of k_1 from the asymptote of the hyperbola). The initial binding velocity as a function of

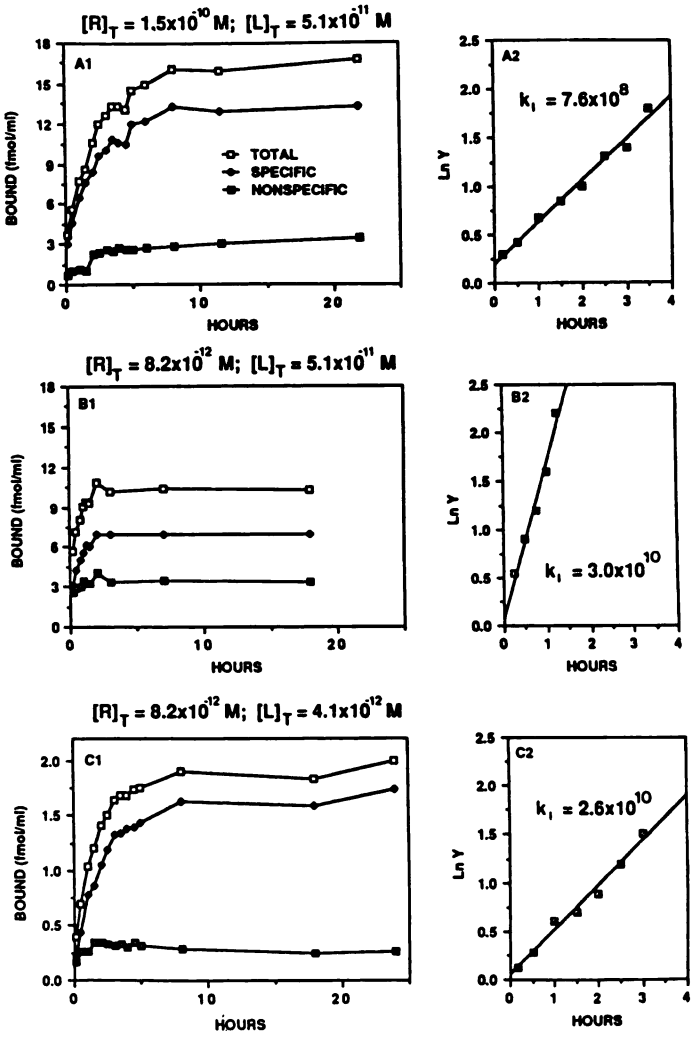

Fig. 6. Time course of association of [^{125}I]2-iodo-7,8dibromodibenzo-*p*-dioxin to the hepatic *Ah* receptor at 4°: estimate of the association rate constant. The time course of ligand receptor association was monitored at receptor concentrations of 1.5×10^{-10} M and 8.2×10^{-12} M (ASPPT fraction equal to protein concentrations of 1160 and 72 μg/ml) and radioligand concentrations of 5.1×10^{-11} M and 4.1×10^{-12} M (250,000 and 20,000 dpm/ml). Each *point* represents the average of two determinations. The data are presented as a plot of bound radioligand as a function of time (A1, B1, and C1), and as a plot of ln*Y* (left side of Eq. 3) as a function of time (A2, B2, and C2). The rate constant of association was determined from the slope of ln*Y* versus time plots as described in Eq. 4 and is inset (units of M^{-1} hr^{-1}).

radioligand concentration, at a fixed receptor concentration of 6.8×10^{-12} M, is shown in Fig. 7B. This plot yielded a good linear fit and an estimate of the second order rate constant of association equal to 5×10^{10} M^{-1} hr^{-1}.

Dissociation rate constants. As shown in Figs. 8 and 9, the dissociation of the ligand-receptor complex does not follow a simple first-order process. The dissociation profile is independent of the receptor concentration or the type of preparation. The data is best fit by a two-component exponential curve ($y = Ae^{k_1 t} + Be^{k_2 t}$).[2] The initial rapidly dissociating component comprises approximately 75% of the total complex and has a

[2] Our results indicate that a statistically better fit was obtained by using a biexponential model over a monoexponential one ($p < 0.001$). We used the partial *F* test as described by Munson and Rodbard (15). No further improvement was obtained when attempts were made to fit the data to a triexponential model ($p < 0.98$), although this and higher order exponential models cannot be ruled out by the data presented.

MOL PHARM
MOLECULAR PHARMACOLOGY
aspet
Downloaded from molpharm.aspetjournals.org at Universidade do Estado do Rio de Janeiro on December 4, 2012

TABLE 2

Summary of kinetic data

Rate constants were calculated as described in the text and expressed as the mean and, where possible, the standard error. The equilibrium dissociation constant, K_D, was determined by 1) Scatchard analysis of the saturation binding isotherm at infinite dilution (Fig. 3) or 2) as a ratio of the dissociation rate constant, k_{-1} (0.36 hr^{-1}) and the association rate constant from either the integrated rate equation or the initial binding velocity method. The dissociation rate constants presented above have not been corrected for receptor-ligand complex destruction rates, thus they are the sum of dissociation and destruction rates (see Results).

	L_T	R_T	k_1
	M	M	$M^{-1}\ hr^{-1}$
Association rate constant			
Integrated 2nd-order	4.1×10^{-12}	8.2×10^{-12}	2.6×10^{10}
	5.1×10^{-11}	8.2×10^{-12}	3.0×10^{10}
	5.1×10^{-11}	1.5×10^{-10}	7.6×10^{8}
Initial velocity method			
Ligand	2.1×10^{-11}	Varied	5.5×10^{10}
Receptor	Varied	6.8×10^{-12}	5.0×10^{10}

	k_{-1}	Percent	k_{-2}	Percent
	hr^{-1}		$hr^{-1} \times 10^3$	
Dissociation rate constant				
ASPPT	0.37 ± 0.02	78 ± 4	4.3 ± 0.4	22 ± 1
Cytosol	0.36 ± 0.05	77 ± 7	9.4 ± 0.8	23 ± 2
Warmed cytosol	0.36 ± 0.04	72 ± 5	7.2 ± 0.5	28 ± 1

	K_D
	M
Equilibrium dissociation constant	
Scatchard (infinite dilution)	$6.0 \pm 3 \times 10^{-12}$
Kinetic (initial velocity)	6.9×10^{-12}
Kinetic (integrated 2nd order)	13.0×10^{-12}

dissociation rate of 0.36 hr^{-1} ($t_{1/2}$ = 1.9 hr). The second slower dissociating component (25%) has a rate constant of 4.3 to 9.4 $\times 10^{-3}$ hr^{-1} ($t_{1/2}$ = 74–161 hr) (Table 2). The rate constant for "degradation"[3] of the receptor-ligand complex at 4° is ~2 $\times 10^{-3}$ hr^{-1}, monoexponential for over 120 hr, and not significantly affected by protein concentration. Thus, the second component of "dissociation" is a composite, representing both ligand-receptor dissociation and degradation. The rate constant for degradation of the unoccupied receptor is ~4 $\times 10^{-3}$ hr^{-1} and is monoexponential for over 100 hr.

As shown in Table 2, K_D values calculated as the ratio of kinetic constants, k_{-1}/k_1 (where k_{-1} is the dissociation rate constant of the major rapid dissociating pool and k_1 is estimated from the integrated second-order equation or initial velocity method), are 6.9×10^{-12} and 13.0×10^{-12} M, which agree very well with the K_D determined by equilibrium saturation data extrapolated to infinite dilution, 6.0×10^{-12} M.

Discussion

Due to its high receptor affinity, high biological potency, commercial availability, and environmental importance, TCDD has become the most studied *Ah* receptor ligand. Despite extensive characterization of the *Ah* receptor using [^{3}H]TCDD or other ligands, no detailed kinetic analysis of ligand-receptor binding has appeared. The kinetic and equilibrium studies in this report challenge the following two assumptions implicit in past binding studies: 1) that both specifically bound radioligand and free radioligand concentrations can be determined accurately at high protein concentrations and 2) that ligand-*Ah* receptor binding can be described by a simple reversible bimolecular model (Eq. 1).

The most common method of analyzing equilibrium saturation binding data is the linear transformation of Scatchard (17):

$$\frac{[LR]}{[L]} = \frac{[R]_T - [LR]}{K_D} \quad (7)$$

or

$$\frac{[\text{Bound}]}{[\text{Free}]} = -\frac{1}{K_D}[\text{Bound}] + \frac{B_{max}}{K_D} \quad (8)$$

A plot of the ratio of specifically bound ligand/free ligand as a function of specifically bound permits one to estimate K_D and total binding sites, $[R]_T$. Analysis of equilibrium binding data by the Scatchard equation requires that a number of criteria be met as follows: 1) the concentration of specifically bound and free ligand are measured accurately at equilibrium; 2) both ligand and receptor are homogenous species; 3) binding obeys the law of mass action as described in Eq. 1 and 2; and 4) no cooperativity exists.

Criterion 1: Measurement of free and specifically bound ligand is accurate. The accuracy of K_D and B_{max} values generated from Eq. 8 is dependent upon the accuracy of the determination of bound and free. Estimates of bound radioligand are fairly straightforward and can be supported by physicochemical characterization of the ligand-receptor complex (e.g., density gradient centrifugation, size exclusion chromatography, anion exchange chromatography, etc.). Conversely, the concentration of free radioligand is most often determined indirectly as the difference between total radioligand in solution and total bound radioligand. In *Ah* receptor-ligand binding studies, free is defined operationally as the amount of radioactivity that can be adsorbed to charcoal (20), that can be removed from hydroxyapatite by extensive detergent washing (21), or that does not sediment in a sucrose gradient (22). By these methods, radioligand, bound to low affinity nonspecific binding sites, that dissociates during charcoal adsorption, hydroxyapatite washing, or long-term centrifugation will be misclassified as free radioligand. This systematic misclassification will decrease the ratio of bound/free ligand and hence decrease the slope of the Scatchard plot (i.e., $-1/K_D$), although it may not significantly compromise estimates of B_{max} (18, 23, 24). One would expect the misclassification of nonspecifically bound radioligand as free radioligand to be greatest, and thus the overestimation of K_D to be greatest, at higher protein concentrations. We believe this is the most plausible explanation of the data presented in Figs. 3–5 and Table 1.

Using [^{3}H]TCDD, Farrel and Safe (25) have noted a relationship between protein concentration and K_D estimates generated from Scatchard analysis of saturation binding data. Characterization of *Ah* receptor ligand binding with a radioligand of modest specific activity, such as [^{3}H]TCDD, necessitates the use of protein concentrations greater than 1 mg/ml (20–22, 25). Thus, K_D values generated previously for [^{3}H]

[3] The degradation rate of the ligand-receptor complex was determined by incubation of the ASPPT fraction (72, 145, and 290 μg of protein/ml) with radioligand with or without 200-fold excess 2,3,7,8-tetrachlorodibenzofuran at 4° for 16 hr (as described in the legend to Fig. 8). Specific binding was determined on aliquots removed at time intervals from 16 to 136 hr. The degradation rate of the unoccupied receptor was estimated by sampling a receptor preparation stored at 4° after various time intervals. The receptor sample was incubated with radioligand with or without 200-fold excess 2,3,7,8-tetrachlorodibenzofuran at 4° for 16 hr, and specifically bound radioligand was determined. The degradation rates were estimated from the plots of the log of specific binding versus time.

MOL PHARM
MOLECULAR PHARMACOLOGY
aspet
Downloaded from molpharm.aspetjournals.org at Universidade do Estado do Rio de Janeiro on December 4, 2012

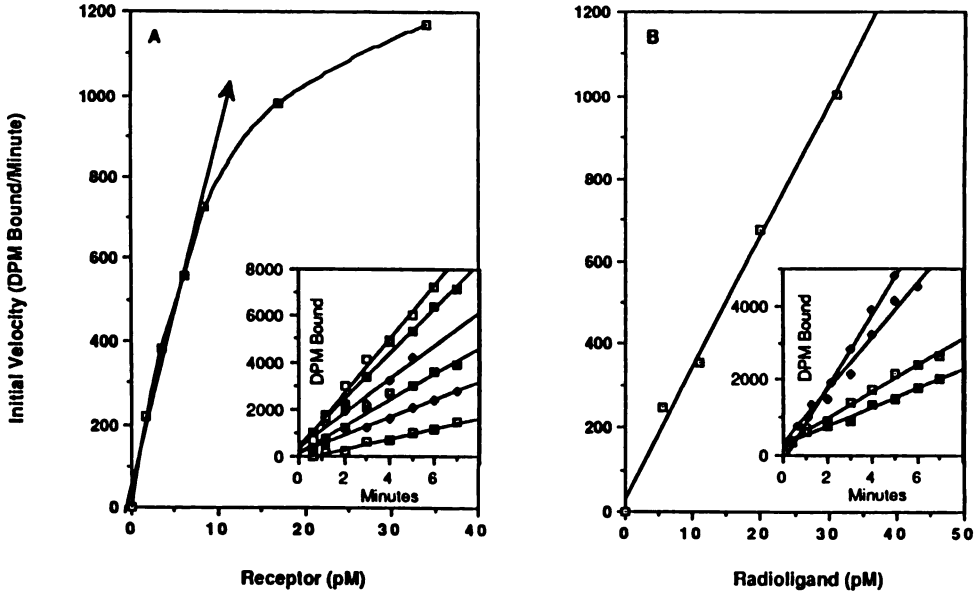

Fig. 7. Initial binding velocity of [^{125}I]2-iodo-7,8-dibromodibenzo-*p*-dioxin to the hepatic *Ah* receptor: estimate of the association rate constant. The ASPPT fraction in MDENG buffer was incubated with radioligand in 50-ml Ehrlenmeyer flasks. At the indicated times intervals, 1.0-ml aliquots were transferred to borosilicate tubes containing 1000-fold molar excess of 2,3,7,8-tetrachlorodibenzofuran (800-fold for nonspecific binding) to prevent further binding of the radioligand and total, specifically, and nonspecifically bound radioligand was determined. Receptor concentrations were determined by duplicate Scatchard analyses. A, Initial binding velocity as a function of *Ah* receptor concentration. Receptor concentrations of 1.7×10^{-12} M (⊡), 3.4×10^{-12} M (♦), 6.1×10^{-12} M (▣), 8.5×10^{-12} M (◇), 1.7×10^{-11} M (■), and 2.4×10^{-11} M (□) were incubated with a fixed radioligand concentration, 2.7×10^{-11} M. The initial binding velocity was determined for each receptor concentration from the slope of the plot of specifically bound radioligand as a function of time (*inset*). The initial binding velocities were then plotted as a function of receptor concentration. The rate constant of association was calculated from the slope of the linear portion of the line (asymptote of the hyperbola) divided by the ligand concentration (see Materials and Methods). B, Initial binding velocity as a function of radioligand concentration. A fixed concentration of receptor, 6.8×10^{-12} M, was incubated with radioligand concentrations of 5.6×10^{-12} M (▣), 1.1×10^{-11} M (⊡), 2.0×10^{-11} M (♦), and 3.1×10^{-11} M (◇). The initial binding velocity was calculated from the slope of specifically bound radioligand as a function of time (*inset*). The initial velocity was plotted as a function of radioligand concentration. The rate constant of association was calculated from the slope of this line divided by the receptor concentration.

TCDD are probably overestimates. Using a competitive binding assay with [^{125}I]2-iodo-7,8-dibromodibenzo-*p*-dioxin as the radioligand and low protein concentration, we estimate the K_D for TCDD to be approximately 4×10^{-12} M.[4]

Misclassification of nonspecifically bound radioligand as free radioligand has been described in a number of other receptor systems that bind hydrophobic ligands: estrogen (23), progesterone (24), and thyroxine (26). In these systems, misclassification errors have been minimized by the use of methods that better estimate free and bound radioligand, e.g., equilibrium dialysis (23, 24) or centrifugal ultrafiltration-dialysis (27). Because our radioligand adsorbs strongly to dialysis tubing and filter membranes,[5] we provided support for radioligand misclassification by the following: 1) demonstrating that addition of a purified protein (BSA) decreases, whereas receptor enrichment increases, the slope of the Scatchard plot (Fig. 5 and Table 1), and 2) eliminating the possibility that the rate constants of association or dissociation were altered by dilution.

We observed that, like K_D, the apparent association rate constant also varies as a function of the concentration of receptor, or more likely, protein (Figs. 6 and 7A). Association rate constant estimates are also dependent upon accurate determination of free radioligand. From the initial velocity rate equation (Eq. 6), it follows that for a given ligand concentration a plot of v_0 as a function of receptor concentration will yield a linear plot, with a slope equal to $k_1[L]_T$. The hyperbolic shape of the curve generated (Fig. 6A) indicates that $k_1[L]_T$ is decreasing as the concentration of the receptor preparation increases and supports the idea that free is being overestimated at higher receptor concentrations. An alternative explanation is that k_1 is actually increasing with dilution of the receptor. Because k_1 is a function of diffusion rate and the energy of activation for the binding step (28), an increase in k_1 with dilution implies that a decrease in the energy of activation for ligand binding is also occurring with dilution. A decrease in the energy of activation for the forward reaction should also result in a decrease in the energy of activation for the dissociation reaction and lead to a increasing k_{-1} with dilution. Because k_{-1} is not affected by protein concentration (Fig. 7 and discussion below), the hyperbolic nature of the curve depicted in Fig. 6A is best explained by an overestimation of free radioligand at the higher protein concentrations.

Criterion 2: Both ligand and receptor are homogenous binding species. The time course of ligand-receptor dissociation is biphasic, suggesting two ligand-receptor species that have dissociation rate constants differing by a factor of at least 60-fold (Figs. 8 and 9 and Table 2). The dissociation of [^{3}H]TCDD from the rat *Ah* receptor has previously been described as "irreversible" (25). Our preliminary comparisons between the dissociation kinetics of the *Ah* receptor-radioligand complex in the Harlan-Sprague Dawley rat and C57BL/6J mouse indicate significant differences.[5]

Criterion 3: Binding obeys the law of mass action as described in Eq. 1. The linear functions generated from plots of initial binding velocity (v_0) versus either the ligand or

[4] C. A. Bradfield and A. Poland, manuscript in preparation.
[5] C. A. Bradfield, and A. Poland, unpublished observations.

MOL PHARM
MOLECULAR PHARMACOLOGY
aspet
Downloaded from molpharm.aspetjournals.org at Universidade do Estado do Rio de Janeiro on December 4, 2012

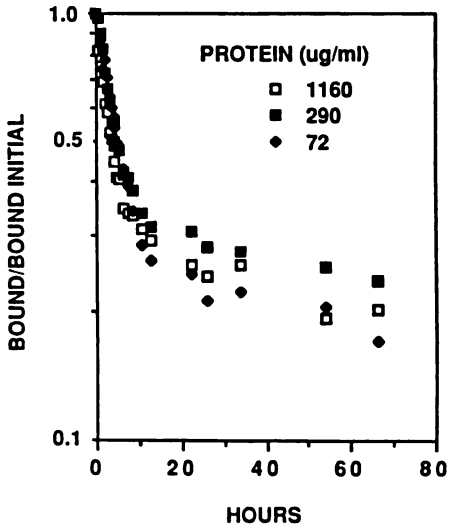

Fig. 8. Dissociation of the [^{125}I]2-iodo-7,8-dibromodibenzo-*p*-dioxin *Ah* receptor complex at 4°: the effect of protein concentration. Radioligand-receptor complexes were preformed by incubation of radioligand and receptor for 16 hr at 4° in 50-ml Ehrlenmeyer flasks. Fractional receptor occupancy of radioligand was between 15 and 18% for all protein concentrations. This was achieved by the following protein (receptor) and radioligand concentrations: 1160 μg/ml (150 pM) and 62 pM; 290 μg/ml (35 pM) and 15 pM; and 72 μg/ml (8.2 pM) and 4 pM. After equilibrium binding had been obtained, a 1000-fold excess of 2,3,7,8-tetrachlorodibenzofuran was added to prevent rebinding of radioligand (time zero). Bound radioligand was determined, at the indicated times, on 1.0-ml aliquots. Nonspecific binding was determined by the addition of a 200-fold excess of 2,3,7,8-tetrachlorodibenzofuran during the pre-binding stage, followed by the addition of an 800-fold excess at time zero. All values were determined in duplicate. Results are presented as specifically bound radioligand/radioligand specifically bound at time zero, plotted as a function of time.

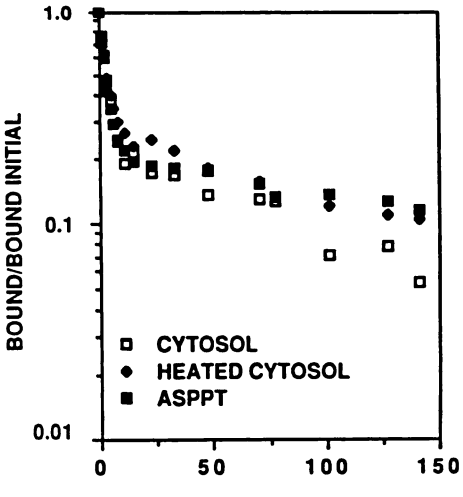

Fig. 9. Dissociations of [^{125}I]2-iodo-7,8-dibromodibenzo-*p*-dioxin from different receptor preparations at 4°. Dissociation rates were determined as described in Fig. 6. *Cytosol* (85 μg of protein/ml) and ASPPT (72 μg/ml) were preincubated with 10 pM radioligand for 16 hr at 4° before dissociation rate determinations. *Heated cytosol* was preincubated for 18 hr at 4° as above, followed by a 30-min incubation at 30°, then recooled to 4° (30 min) before dissociation rate determination. Kinetic rate constants were calculated by the nonlinear curve fitting technique, constrained to a biexponential model, as described (16).

receptor concentrations (Fig. 7) indicate that the binding reaction is first order with respect to both radioligand and receptor and thus second order overall (formation of the ligand receptor complex) (28). This lends support to the assumption that one molecule of ligand binds to one molecule of receptor.

Biphasic ligand-receptor dissociation is not in agreement with the equilibrium binding scheme presented in Eq. 1. Biphasic ligand-receptor dissociation curves have been observed for ligands bound to the estrogen (29, 30), progesterone (31), glucocorticoid (32), and androgen (33) receptors. For these steroid hormone receptors, the slow dissociating species (believed to represent a "transformed" receptor species) has an increased affinity for polyanionic matrices such as DNA (33–35) and an altered molecular mass as compared with the fast dissociating species (36, 37). In these systems, in which the ratio of the fast to slow component can be altered by increasing the ionic strength, heating, etc., we did not observe a significant change in the ratio of the fast and slow components by heating a 30° for 30 min, dilution, or ammonium sulfate precipitation.

Ligand binding to the *Ah* receptor appears to conform to the model proposed for the steroid hormone receptor (32) in which:

$$L + R \underset{k_{-1}}{\overset{k_1}{\leftrightarrows}} LR \underset{k_{-12}}{\overset{k_{12}}{\leftrightarrows}} LR' \underset{k_{-2}}{\overset{k_2}{\leftrightarrows}} L + R' \qquad (9)$$

and thus at equilibrium:

$$K_D = \frac{[L]\,[R]}{[LR] + [LR']} \qquad (10)$$

Criterion 4: No site-site cooperatively exists. Hill coefficients were 1.0 at all dilutions; there is no indication of cooperativity in this system. Hill coefficients of approximately 1.0 have previously been reported for a number of mammalian species (25, 38).

In this report, analysis of the *Ah* receptor-ligand binding, facilitated by a new high specific activity radioligand has revealed important findings. 1) Estimates of the apparent K_D, as determined by Scatchard analysis, are a function of protein concentration and attributable to a systematic overestimation of free ligand. The true K_D (from equilibrium saturation at infinite dilution and ratio of kinetic constants k_{-1}/k_1) is approximately 100 times lower than previous estimates. 2) The *Ah* receptor ligand complex can exist as two distinct species, which have different dissociation rates, and thus ligand binding does not conform to a simple reversible mass action model, as has been assumed previously.

References

1. Poland, A., and J. C. Knutson. 2,3,7,8-Tetrachlorodibenzo-*p*-dioxin and related halogenated aromatic hydrocarbons: examination of the mechanism of toxicity. *Annu. Rev. Pharmacol. Toxicol.* **22**:517–554 (1982).
2. Whitlock, J. P. The regulation of cytochrome P-450 gene expression. *Annu. Rev. Pharmacol. Toxicol.* **26**:333–369 (1986).
3. Greenlee, W. F., and A. Poland. Nuclear uptake of the 2,3,7,8-tetrachlorodibenzo-*p*-dioxin in C57BL/6J and DBA/2J mice. *J. Biol. Chem.* **254**:9814–9821 (1979).
4. Okey, A. B., G. P. Bondy, M. E. Mason, G. F. Kahl, H. J. Eisen, T. M. Guenther, and D. W. Nebert. Regulatory gene product of the *Ah* locus: characterization of the cytosolic inducer-receptor complex and evidence for its nuclear translocation. *J. Biol. Chem.* **254**:11636–11648 (1979).
5. Hannah, R. R., J. Lund, L. Poellinger, M. Gillner, and J.-A. Gustafsson. Characterization of the DNA-binding properties of the receptor for 2,3,7,8-tetrachlorodibenzo-*p*-dioxin. *Eur. J. Biochem.* **156**:237–242 (1986).
6. Gasiewicz, T. A., and P. A. Bauman. Heterogeneity of the rat *Ah* receptor and evidence for transformation *in vitro* and *in vivo*. *J. Biol. Chem.* **262**:2116–2120 (1987).
7. Jones, P. B. C., L. K. Durrin, J. M. Fisher, and J. P. Whitlock. Control of gene expression by 2,3,7,8-tetrachlorodibenzo-*p*-dioxin: multiple dioxin-re-

MOL PHARM
MOLECULAR PHARMACOLOGY
aspet
Downloaded from molpharm.aspetjournals.org at Universidade do Estado do Rio de Janeiro on December 4, 2012

sponsive domains 5′-ward of the cytochrome P_1-450 gene. *J. Biol. Chem.* **261**:6647–6650 (1986).
8. Giguere, V., S. M. Hollenberg, M. G. Rosenfeld, and R. M. Evans. Functional domains of the human glucocorticoid receptor. *Cell* **46**:645–652 (1986).
9. Denison, M. S., L. M. Vella, and A. B. Okey. Structure and function of the *Ah* receptor for 2,3,7,8-tetrachlorodibenzo-*p*-dioxin. *J. Biol. Chem.* **261**:3987–3995 (1986).
10. Vedeckis, W. V. Steroid hormone receptor structure in normal and neoplastic cells, in *Hormonally Responsive Tumors* (V. P. Hollander, ed). Academic Press, New York, 4–55 (1985).
11. Poland, A., E. Glover, F. H. Ebitino, and A. S. Kende. Photoaffinity labeling of the *Ah* receptor. *J. Biol. Chem.* **261**:6352–6365 (1986).
12. Denny, J. B., and G. Blobel. ^{125}I-Labeled crosslinking reagent that is hydrophylic, photoactivatable, and cleavable through an azo linkage. *Proc. Natl. Acad. Sci. USA* **81**:5286–5290 (1984).
13. Cadogan, J. I. G., and G. A. Molina. A simple and convenient deamination of aromatic amines. *J. Chem. Soc. Perkins Trans I* 541–542 (1973).
14. Warburg, O. and, W. Christian. Isolierung und kristallisation des gärungsferments enolase. *Biochem. Z.* **310**:384–421 (1942).
15. Munson, P. J., and D. Rodbard. Ligand: a versatile computerized approach for characterization of ligand-binding systems. *Anal. Biochem.* **107**:220–239 (1980).
16. McPherson, G. A. Analysis of radioligand binding experiments: a collection of computer programs for the IBM PC. *J. Pharmacol. Methods* **14**:213–228 (1985).
17. Scatchard, G. The attractions of proteins for small molecules and ions. *Ann. N. Y. Acad. Sci.* **51**:660–672 (1949).
18. Bennet, J. P., and H. I. Yamamura. Neurotransmitter, hormone, or drug receptor binding methods, in *Neurotransmitter Receptor Binding* (H. I. Yamamura, S. J. Enna, and M. J. Kuhar, eds). Raven Press, New York, 61–90 (1985).
19. Weiland, G. A., and P. B. Molinoff. Quantitative analysis of drug-receptor interactions. I. Determination of kinetic and equilibrium properties. *Life Sci.* **29**:313–330 (1981).
20. Poland, A., and E. Glover. 2,3,7,8-Tetrachlorodibenzo-*p*-dioxin: segregation of toxicity with the *Ah* locus. *Mol. Pharmacol.* **17**:86–94 (1979).
21. Gasiewicz, T. A., and R. A. Neal. The examination and quantitation of tissue cytosolic receptors for 2,3,7,8-tetrachlorodibenzo-*p*-dioxin using hydroxylapatite. *Anal. Biochem.* **124**:1–11 (1982).
22. Manchester, D. K., S. K. Gordon, S. L. Golas, E. A. Roberts, and A. B. Okey. *Ah* receptor in human placenta: stabilization by molybdate and characterization of binding of 2,3,7,8-tetrachlorodibenzo-*p*-dioxin, 3-methylcholanthrene, and benzo(*a*)pyrene. *Cancer Res.* **47**:4861–4868 (1987).
23. Siiteri, P. K. Receptor binding studies. *Science (Wash. D. C.)* **223**:191–193 (1984).
24. Saiduddin, S., and H. P. Zassenhaus. *In vitro* and *in vivo* enhancement of progesterone binding to the uterine progesterone receptor by cortisol. *Biochemistry* **16**:2829–2834 (1977).
25. Farrel, K., and S. Safe. Absence of positive cooperativity in the binding of 2,3,7,8-tetrachlorodibenzo-*p*-dioxin to its cytosolic receptor protein. *Biochem. J.* **244**:539–546 (1987).
26. Seelig, S., H. L. Schwartz, and J. H. Oppenheimer. Limitations in the conventional analysis of the interaction of triiodothyronine with solubilized nuclear receptor sites. *J. Biol. Chem.* **256**:2154–2161 (1981).
27. Hammond, G. L., J. A. Nisker, L. A. Jones, and P. K. Siiteri. Estimation of the percentage of free steroid in undiluted serum by centrifugal ultrafiltration dialysis. *J. Biol. Chem.* **255**:5023–5026 (1980).
28. Meites, L. An introduction to chemical kinetics, in *An Introduction to Chemical Equilibrium and Kinetics*. Pergamon Press, New York, 33–76 (1981).
29. Best-Belpomme, M., J. Fries, and T. Erdos. Interactions entre l'oestradiol et des sites récepteurs utérins. *Eur. J. Biochem.* **17**:425–432 (1970).
30. Best-Belpomme, M., J. Mester, H. Weintraub, and E.-E. Baulieu. Oestrogen receptors in chick oviduct: characterization and subcellular fractionation. *Eur. J. Biochem.* **57**:537–547 (1975).
31. Wolfson, A., J. Mester, Y. Chang-Ren, and E.-E. Baulieu. Non-activated form of the progesterone receptor from chick oviduct: characterization. *Biochem. Biophys. Res. Commun.* **95**:1577–1584 (1980).
32. Pratt, W. B., J. L. Kaine, and D. V. Pratt. The kinetics of glucocorticoid binding to the soluble specific binding protein of mouse fibroblasts. *J. Biol. Chem.* **250**:4584–4591 (1975).
33. de Boer, W., M. Lindh, J. Bolt, A. Brinkmann, and E. Mulder. Characterization of the calf uterine androgen receptor and its activation to the deoxyribonucleic acid-binding state. *Endocrinology* **118**:851–861 (1986).
34. McBlain, W. A., D. O. Toft, and G. Shyamala. Transformation of mammary cytoplasmic glucocorticoid receptor under cell-free conditions. *Biochemistry* **20**:6790–6798 (1981).
35. Yang, C. R., J. Mester, A. Wolfson, J. M. Renoir, and E.-E. Baulieu. Activation of the chick oviduct progesterone receptor by heparin in the presence or absence of hormone. *Biochem. J.* **208**:399–406 (1982).
36. Weichman B. M., and A. C. Notides. Estradiol-binding kinetics of the activated and nonactivated estrogen receptor. *J. Biol. Chem.* **252**:8856–8862 (1977).
37. Muller, R. E., D. M. Beebe, E. Bercel, A. M. Traish, and H. H. Wotiz. Estriol and estradiol interactions with the estrogen receptor *in vivo* and *in vitro*. *J. Steroid Biochem.* **20**:1039–1046 (1984).
38. Gasiewicz, T. A., and G. Rucci. Cytosolic receptor for 2,3,7,8-tetrachlorodibenzo-*p*-dioxin: evidence for a homologous nature along mammalian species. *Mol. Pharmacol.* **26**:90–98 (1984).

Send reprint requests to: Alan Poland, McArdle Laboratory for Cancer Research, University of Wisconsin, Madison, WI 53706.

MOL PHARM
MOLECULAR PHARMACOLOGY
aspet
Downloaded from molpharm.aspetjournals.org at Universidade do Estado do Rio de Janeiro on December 4, 2012